Journal of Catalysis **202,** 245–255 (2001)
doi:10.1006/jcat.2001.3278, available online at http://www.idealibrary.com on IDEAL®

A Novel Titanosilicate with MWW Structure: II. Catalytic Properties in the Selective Oxidation of Alkenes

Peng Wu,* Takashi Tatsumi,*[,1] Takayuki Komatsu,† and Tatsuaki Yashima†

**Division of Materials Science & Chemical Engineering, Graduate School of Engineering, Yokohama National University,*
79-5 Tokiwadai, Hodogaya-ku, Yokohama 240-8501, Japan; and †Department of Chemistry, Tokyo
Institute of Technology, 2-12-1 Ookayama, Meguro-ku, Tokyo 152-8551, Japan

Received January 9, 2001; revised May 14, 2001; accepted May 14, 2001; published online August 9, 2001

The catalytic properties of Ti–MWW catalysts have been studied for the oxidation of alkenes using hydrogen peroxide or *tert*-butyl hydroperoxide (TBHP) as an oxidant. Ti–MWW shows superior activity independent of the nature of oxidant when compared to the other Ti-containing catalysts both of microporous TS-1 and Ti-MOR and of mesoporous Ti–MCM-41 in the oxidation of cyclohexene. Compared to large-pore Ti–Beta, Ti–MWW is less active than in the oxidation of cyclohexene using H_2O_2, but its shows comparable activity in the case of TBHP. Ti–MWW is very stable in both the structure and the states of Ti species in the actual cycle of reaction–regeneration. The framework B species remaining within the Ti–MWW catalysts seem to have little influence on the intrinsic activity of framework Ti species, but they act as Brønsted acid sites contributing to the hydrolysis of the oxide product to form glycols. The turnover number (TON) of Ti–MWW for the cyclohexene conversion decreases sharply with increasing Ti content, while the TON for the 1-hexene conversion shows volcanic behavior when related to the Ti content. It is clarified that the bulky reaction is catalyzed mainly by the Ti species within the supercages and the exterior pockets of the MWW structure, while in addition to these highly accessible Ti species, those within the channels of a 10-membered ring greatly contribute to the oxidation reactions not significantly sizedemanding. © 2001 Academic Press

INTRODUCTION

A breakthrough has occurred in the field of zeolite catalysis since a group at EniChem synthesized the MFI-type titanosilicate, TS-1, which can be used as an oxidation catalyst in the liquidphase (1, 2). A major disadvantage of TS-1 is that it is limited in catalyzing the reactions of the substrates with relatively small molecular sizes due to the medium pores of a 10-membered ring. This stimulates the researchers to prepare the Ti-containing zeolites with larger pores, such as Ti–Beta (3, 4), TAPSO-5 (5), Ti–MOR (6), and ITQ-7 (7) either by direct hydrothermal synthesis or by secondary solid–gas reaction using $TiCl_4$ vapor. There is still room for preparing Ti-containing zeolites with more accessible Ti sites which are able to catalyze the bulky reactions in the fields of fine chemicals and pharmaceuticals. Mesoporous Ti–MCM-41 developed recently has been greatly expected to be a potentially useful catalyst by zeolite chemists from this point of view, but it faces the serious problems of low stability in both the structure and Ti species (8–10). Recently (11), we succeeded in preparing a Ti-containing zeolite with MWW topology, Ti–MWW, by combining hydrothermal synthesis and subsequent acid treatment. It is hoped this material can expand the potential applications of titanosilicates because the MWW structure has the supercages within the crystals and the pockets on the exterior (12) and also that the MWW-type lamellar precursor can be converted into a micro-mesoporous hybrid (13) or can be delaminated into thin sheets (14), both the materials having the reaction space highly accessible to the bulky molecules.

In this study, we have investigated the catalytic properties of Ti–MWW in the selective oxidation of alkenes with different molecular sizes using *tert*-butylhydroperoxide (TBHP) or hydrogen peroxide as an oxidant. The main issues are to clarify the catalytic behavior of the differently located Ti sites derived from the unique structure of MWW topology and to investigate the stability of the Ti species toward the reaction. Since Ti–MWW contains boron atoms within its framework to various levels depending on the preparation conditions (11), the influence of the framework composition on the intrinsic activity of the Ti sites and the product selectivity has also been studied.

EXPERIMENTAL

Catalysts Preparation and Characterization

Ti–MWW catalysts with various Ti contents were prepared as reported previously (11). The lamellar precursors, denoted as Ti–MWW–PI(n) and Ti–MWW–HM(n) where n is the Si/Ti ratio of gel, were synthesized from the gels

---

[1] To whom correspondence should be addressed. Fax: +81-45-339-3941. E-mail: ttatsumi@ynu.ac.jp.

0021-9517/01 $35.00

TABLE 1

Preparation Conditions and Physico-chemical Properties of Ti–MWW Catalysts

	Acid treatment conditions[a]		Composition[b]		Surface area		Crystal size[d] (μm)	
No.	Parent used	Acid concen.	Si/B	Si/Ti	(m^2 g^{-1})	Ti species[c]	Thickness	Length
1	B–MWW–PI	No treatment	11.8	∞	616	Ti-free	—[e]	
2	No. 1 + 6 M HNO_3	6 M HNO_3	694	∞	627	Ti-free	—[e]	
3	Ti–MWW–PI(100)	2 M HNO_3	34	146	—[e]	Tetra..	0.05–0.1	0.2–0.5
4	Ti–MWW–PI(100)	6 M HNO_3	95	183	621	Tetra.	0.05–0.1	0.2–0.5
5	No. 3	2 M HNO_3	489	203	635	Tetra.	0.05–0.1	0.2–0.5
6	Ti–MWW–PI(70)	6 M HNO_3	74	116	622	Tetra.	—[e]	
7	No. 6	2 M HNO_3	625	136	623	Tetra.	—[e]	
8	Ti–MWW–PI(50)	1 M HNO_3	36	63	626	Tetra.	0.05–0.1	0.2–0.5
9	Ti–MWW–PI(50)	2 M HNO_3	39	72	624	Tetra.	0.05–0.1	0.2–0.5
10	Ti–MWW–PI(50)	6 M HNO_3	89	131	615	Tetra.	0.05–0.1	0.2–0.5
11	Ti–MWW–PI(50)	2 M H_2SO_4	48	76	—[e]	Tetra.	0.05–0.1	0.2–0.5
12	Ti–MWW–PI(50)	18 M H_2SO_4	83	457	628	Tetra.	0.05–0.1	0.2–0.5
13	No. 9	2 M HNO_3	543	107	—[e]	Tetra.	0.05–0.1	0.2–0.5
14	No. 9	6 M HNO_3	553	136	631	Tetra.	0.05–0.1	0.2–0.5
15	Ti–MWW–PI(30)	2 M H_2SO_4	36	47	—[e]	Tetra..	0.05–0.1	0.2–0.5
16	Ti–MWW–PI(30)	2 M HNO_3	49	46	628	Tetra.	0.05–0.1	0.2–0.5
17	No. 15	2 M HNO_3	559	59	624	Tetra.	0.05–0.1	0.2–0.5
18	Ti–MWW–PI(20)	2 M HNO_3	54	38	—[e]	Tetra. + Ana.(low)	—[e]	
19	No. 18	2 M HNO_3	476	53	556	Tetra. + Ana.(low)	—[e]	
20	Ti–MWW–PI(10)	2 M H_2SO_4	50	17	543	Tetra. + Octa. + Ana.	0.05–0.1	0.2–0.5
21	No. 20	6 M HNO_3	531	25	548	Tetra. + Octa. + Ana.	0.05–0.1	0.2–0.5
22	Ti–MWW–HM(100)	6 M HNO_3	49	177	543	Tetra.	0.1–0.2	1–1.5
23	Ti–MWW–HM(70)	2 M HNO_3	54	134	625	Tetra.	—[e]	
24	Ti–MWW–HM(50)	2 M HNO_3	50	129	629	Tetra.	0.1–0.2	1–1.5
25	Ti–MWW–HM(30)	6 M HNO_3	37	62	621	Tetra.	0.1–0.2	1–1.5

[a] Other conditions: temp., 373 K; time, 20 h; the ratio of solid to solution, 1 g : 20 ml.

[b] After calcination at 803 K for 10 h.

[c] By UV–visible spectroscopy, Tetra. = tetrahedral, Octa. = octahedral, and Ana. = anatase.

[d] By SEM.

[e] Not determined.

of Si/Ti = 10–∞ and Si/B = 0.75 using piperidine (PI) or hexamethylenenimine (HM) as a structural directing agent (SDA). The acid treatment of the precursors with 1–6 M HNO_3 or 2–18 M H_2SO_4 was carried out to remove the extraframework Ti and the framework B species. Subsequent calcination at 803 K for 10 h led us to obtain the objective Ti–MWW catalysts. In some cases further acid treatment was conducted to prepare the nearly B-free samples. The details for the acid treatment are summarized in Table 1 for a part of the samples.

For comparison, TS-1, Ti–MOR, Ti–Beta, and Ti–MCM-41 were also prepared. TS-1 of Si/Ti = 104 and Ti–MCM-41 of Si/Ti = 110 were hydrothermally synthesized according to the methods in Refs. (6d) and (15), respectively, while Ti–MOR of Si/Ti = 120 was obtained by treating a dealuminated mordenite sample (Si/Al = 300) with the $TiCl_4$ vapor at 773 K for 1 h (6). Ti–Beta (Si/Ti = 40, Si/Al = 71) were hydrothermally synthesized according to Ref. (3).

All the catalysts were characterized by inductively coupled plasma (ICP, Rigaku JY38S), X-ray diffraction (XRD, Rigaku Rint 2000), N_2 adsorption (Coulter SA 3100), scanning electron microscopy (SEM, JEOL JSM-T220), and the specotroscopies of UV–visible (Shimadzu UV-2400PC) and IR (Shimadzu FTIR-8100). IR spectra of the pyridine-adsorbed samples were recorded according to the procedures as follows. A self-supported wafer (9.6 mg cm^{-2} thickness) was set in an IR cell sealed with CaF_2 windows, and the wafer was evacuated at 773 K for 1.5 h before the pyridine adsorption. The adsorption was carried out by exposing the wafer to pyridine vapor (1.3 kPa) at 423 K for 0.5 h. The desorption of pyridine was carried out at 423 and 523 K for 1 h, respectively. All the spectra were collected at room temperature.

Catalytic Reaction

The oxidation of alkenes were carried out under vigorous stirring in a glass flask with a condenser. The temperature of the flask was controlled with an oil bath. In a typical run, 10 mmol of alkene, 10 ml of acetonitrile solvent, and 0.05 g of catalyst were mixed in the flask and heated to 363 K under agitation. A desirable amount of oxidant, TBHP (70 wt%) or H_2O_2 (30 wt%), was then added to the mixture to start the reaction. The products were separated by filtration and analyzed with gas chromatography (Shimadzu GC-14B) using a VO-1 capillary column of 50 m and an FID detector. The amount of unconverted H_2O_2 was determined by a standard titration method with 0.1 M $Ce(SO_4)_2$ solution.

RESULTS AND DISCUSSION

Characterization of Ti–MWW

Table 1 shows the preparation conditions and the physico-chemical properties for a part of Ti–MWW samples. The samples were obtained by treating directly the lamellar precursors with HNO_3 or H_2SO_4 solution and following calcination at 803 K as reported previously (11). All the samples contained only the MWW phase and were highly crystalline materials as verified by XRD. UV–visible spectra indicated that the Ti–MWW samples prepared from the precursors with Si/Ti $>$ 30 contained mainly the tetrahedral Ti species, while those prepared from Si/Ti $=$ 20 and 10 contained also a part of anatase phase and octahedral Ti species. The SEM micrographs revealed the hexagonal crystals of thin platelets for both series of Ti–MWW samples. The crystal size was 0.2–0.5 μm in length and 0.05–0.1 μm in thickness for Ti–MWW–PI and approximately 1 $\times$ 0.1 μm for Ti–MWW–HM. Further acid treatment was carried out on the acid pretreated and calcined samples, which resulted in the nearly B-free samples. When the influence of the adsorbed water was eliminated by evacuation at 773 K, the nearly B-free Ti–MWW samples showed the characteristic 960 cm^{-1} IR band, assigned to the stretching vibration of Si–O–Ti bonds in the framework. The 960-cm^{-1} band increased in intensity linearly with the Ti content (11), in agreement with UV–visible spectroscopy, which demonstrated that the Ti species in Ti–MWW of the Si/Ti ratios higher than 40 occupied the tetrahedral framework sites.

Comparison of Ti–MWW with Other Ti-Containing Catalysts in the Oxidation of Cyclohexene

Table 2 compares the catalytic activity of Ti–MWW with that of TS-1, Ti–MOR, Ti–MCM-41, and Ti–Beta in the oxidation of cyclohexene with TBHP or H_2O_2. Cyclohexene was oxidized to produce cyclohexene oxide as a main product, together with 2-cyclohexene-1-ol, 2-cyclohexene-1-one, and glycols as byproducts. Glycols should be the products of the secondary hydrolysis of cyclohexene oxide. In both the reactions with TBHP and H_2O_2, Ti–MWW–PI(50), prepared by directly calcining the precursor without acid treatment, showed lower conversion, lower specific activity per Ti site (TON), and also lower efficiency of oxidant as expected because of the presence of anatase. However, both the conversion and the TON increased greatly by pretreating the precursor with acid solution followed by calcination. The acid-treated sample and the directly calcined one differ in both the chemical composition of Ti and B and the nature of Ti species. The relatively large amount of B contained within Ti–MWW–PI(50) may be related to the difference in the catalytic performance observed, but as we will discuss in detail later, the framework B does not seem to have

TABLE 2

Comparison of the Catalytic Activity of Ti–MWW with That of Other Catalysts in the Oxidation of Cyclohexene

Catalysts[a]	Composition		SA[b]	Cyclohexene oxidation with TBHP[c]						Cyclohexene oxidation with H_2O_2[c]					
	Si/B	Si/Ti		Conv. (mol%)	TON[d]	Product sel. (mol%)		TBHP (mol%)		Conv. (mol%)	TON[d]	Product sel. (mol%)		H_2O_2 (mol%)	
						Oxide	Others[e]	Conv.	Sel.			Oxide	Others[e]	Conv.	Sel.
Ti–MWW–PI(50)	11	51	621	1.4	9	69	31	3.8	81	2.0	13	10	90	6.0	67
No. 9 calcined	39	72	624	4.2	38	80	20	9.3	95	4.7	42	68	32	10.0	94
No. 10 calcined	89	131	615	4.5	71	84	16	9.5	100	4.9	77	72	28	10.9	95
No. 16 calcined	49	46	628	5.5	33	81	19	11.2	95	6.3	37	64	36	13.4	99
No. 18 calcined	54	38	—[f]	5.7	27	85	15	12.9	93	7.1	34	63	37	15.0	95
No. 9 uncalcined	39	72	445	5.8	60	86	14	12.2	100	—[f]	—	—	—	—	—
No. 10 uncalcined	89	131	446	5.5	87	84	16	11.6	98	—[f]	—	—	—	—	—
TS-1	∞	104	564	0.3	3	24	76	0.9	75	0.5	6	87	23	2.6	41
Ti–MOR	200[g]	120	550	1.1	21	80	20	2.6	88	2.9	55	73	27	8.1	75
Ti–Beta	71[g]	40	600	5.7	20	84	16	13.3	90	11.9	56	68	32	34.0	70
Ti–MCM-41	∞	110	1054	1.4	19	71	19	3.5	85	0.4	5	72	28	1.6	54

[a] The numbers correspond to those in Table 1.

[b] SA $=$ surface area in $m^2\ g^{-1}$.

[c] Conditions: cat., 0.05 g; cyclohexene, 10 mmol; TBHP or H_2O_2, 5 mmol; acetonitrile, 10 ml; temp., 333 K; time, 2 h.

[d] In mol (mol of Ti)$^{-1}$.

[e] 2-Cyclohexene-1-ol, 2-cyclohexene-1-one, glycols.

[f] Not determined.

[g] Si/Al molar ratio.

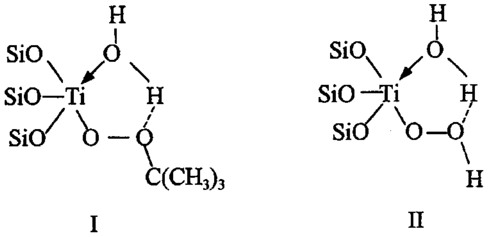

SCHEME 1

a significant influence on the catalytic activity. Concerning the nature of Ti species, the catalyst prepared by directly calcining the precursor always contained the anatase phase as extraframework Ti species (11). These condensed Ti species are generally believed not to catalyze the oxidation of substrates but contribute to the nonproductive decomposition of the oxidant, which retards the catalytic activity of coexistent framework Ti species (1, 2). Therefore, it can be deduced that the catalytically active sites of Ti–MWW are only those tetrahedral Ti species highly dispersed within the framework just like the cases of TS-1 and Ti–Beta.

When Ti–MWW is compared with TS-1, Ti–MOR, and Ti–MCM-41, it is obvious that Ti–MWW is an extremely highly active catalyst for the oxidation of cyclohexene irrespective of the nature of the oxidants. In general, the titanosilicate-catalyzed reactions are believed to involve a cyclic intermediate of a 5-membered ring formed through the coordination of a solvent molecule such as alcohol or H_2O to a Ti peroxo species (16). We have reported that the diffusion rate of aromatics within the channels of both TS-1 and Ti–MOR is about 1 order lower in the presence of H_2O_2 than in the presence of H_2O (11), which further supports the presence of this kind of bulky intermediate. Species I and II shown in Scheme 1 are thus presumed to be the intermediates for TBHP and H_2O_2 oxidations, respectively, since both the oxidants contain water.

Species I is obviously much more bulky than species II due to the *tert*-butyl group. An actual reaction occurs only when the molecules can reach the above intermediates. Therefore, the larger the substrate is, the more open reaction space that is needed. For these reasons, TS-1 reasonably showed the lowest activity for the present reactions due to the serious restrictions expected by its medium pores for both the intermediates. Ti–MOR of the 12-ring channel catalyzed the reaction to a certain level when using a smaller oxidant of H_2O_2, but decreased in activity when both the substrate and the oxidant were bulky molecules. Mesoporous Ti–MCM-41, on the other hand, showed higher activity in the case of TBHP than H_2O_2, which is probably due to its high hydrophilicity preferring use of an organic oxidant (9, 10). In this meaning, the present results suggest that the active sites of Ti–MWW are not mesoporous molecular sieve-like, but fundamentally crystalline zeolite-like.

Ti–Beta showed higher conversion in the case of H_2O_2 than Ti–MWW with a similar Ti content (No. 18 in Table 2), but its activity was retarded seriously for TBHP oxidation. Furthermore, taking account of the fact that not all the Ti species in Ti–MWW can be expected to contribute to the present reactions because of the presence of Ti species in the medium pores, the significant activity of Ti–MWW suggests that it contains the Ti sites easily accessible to bulky molecules.

Acid-pretreated but uncalcined Ti–MWW catalysts showed even slightly higher TON than the calcined one, although the formers had lower surface areas (No. 9 and 10 in Table 2). We have verified previously by the XRD measurements that the lamellar structure turns into the three-dimensional MWW topology partially upon the acid treatment and totally after subsequent calcination (11). The partial construction of the MWW structure during the acid treatment is probably a result of removal of the species supporting the layered sheets. The acid treatment is thus presumed to extract more easily the organic template species and the extraframework Ti species existing between the sheets of the precursors than those species embedded in the 10-membered ring channels within the sheets. For this reason, the acid treatment is enough to open nearly all the space between the sheets, resulting in the catalysts effective for the bulky reactions. Subsequent calcination removes the remaining organic species to open the 10-membered ring channels totally, resulting in a higher surface area; however, the 10-membered ring channels are hardly accessible to the molecules of cyclohexene and TBHP. Conversely, the calcination simultaneously causes total crystallization between the sheets to form supercages regulated by 10-membered ring apertures, which may partially limit the bulky reaction due to steric hindrance. The above results show that even when the calcination procedure is omitted, Ti–MWW is able to effectively catalyze the bulky reaction if only the extraframework Ti species are extracted by acid treatment.

Stability of the Ti Species in Ti–MWW

The stability of the Ti species toward leaching by oxidant or water is directly related to the lifetime of a titanosilicate and the possibility of its reuse when it is adopted as an oxidation catalyst in the liquidphase. TS-1 is believed to be stable toward H_2O_2 solution, in agreement with its well-known catalytic applications such as hydroxylation, epoxidation, and ammoximation (16a). Very recently, Ti–Beta was claimed to be less stable than TS-1 in the H_2O_2 solution (17); extensive cleavage of the Si–O–Ti bonds occurs when Ti–Beta is treated with the H_2O_2 solution, resulting in a highly defective structure. The Ti species thus cleaved may partially go out of the framework during subsequent calcination, forming TiO_2 agglomerates. Furthermore, owing to the abundance of silanol groups which are easily attacked by H_2O, both the structure and the Ti species of Ti–MCM-41

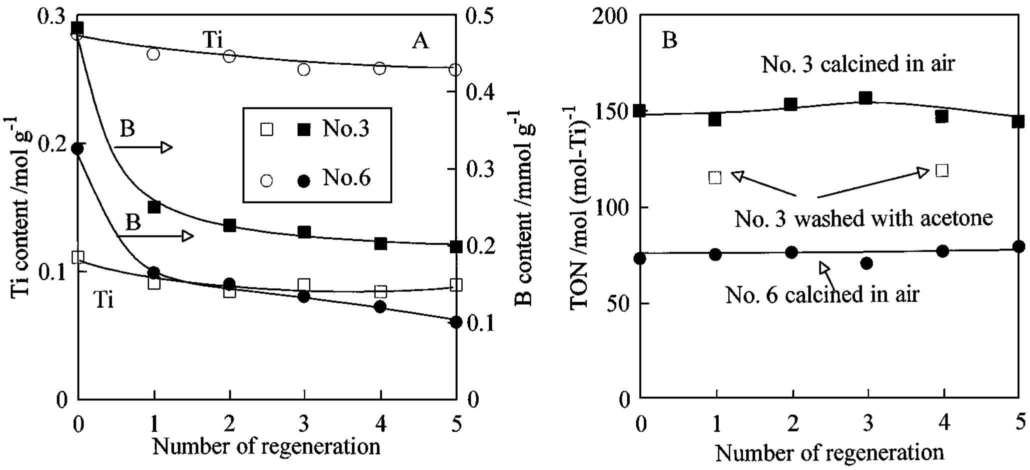

FIG. 1 Changes of the Ti and B contents (A) and that of the TON for the cyclohexene conversion (B) with the cycle of reaction–regeneration. Cyclohexene oxidation: 0.05 g Ti–MWW, 10 mmol of substrate, 5 mmol of H_2O_2, 5 ml of acetonitrile; temp., 333 K; time, 2 h.

are more unstable in the H_2O_2 solution than those of the crystalline zeolites unless its hydrophobicity is enhanced by a silylation of its wall surface (9, 10).

The stability of Ti species of Ti–MWW has been investigated together with that of B species in the oxidation of cyclohexene with H_2O_2. The reaction was repeated on two catalysts with different contents of Ti and B, that is, No. 3 and No. 16 in Table 1. The used catalysts were regenerated either by washing with acetone or by calcining in air. No change in the structure has been observed after the repeated reaction according to the XRD and N_2 adsorption measurements. The changes in the amount of Ti and B upon the regeneration are shown in Fig. 1 where the TON for cyclohexene conversion is also depicted. The B content decreased to nearly half that of the fresh catalyst after the first reaction and further decreased gradually with the reaction–regeneration cycle. The easy leaching of the framework B in the aqueous solution is probably due to a too small radii of B cation, which weakens the Si–O–B bond and makes it cleaved readily by the attack of water to form defect sites in the framework. Although a slight decrease in the Ti content was observed after the first reaction, thereafter, the Ti species in Ti–MWW were stable enough to resist the leaching by H_2O_2, even after five cycles of the reaction–regeneration. The slight leaching of Ti species is probably due to a local rearrangement of the framework occurring in the vicinity of B cations since removing a large amount of B would leave the vacancy and then cause short-range flexibility within the framework. Subsequent calcination partially mends the defect sites, e.g., hydroxyl nests through the dehydroxylation to result in a firm framework and, thus, the stabilization of Ti species. When the used catalyst was regenerated only by washing with acetone, the activity of the Ti species was recovered by about 75%. However, in agreement with the stability of the Ti species, TON was totally restored by burning off the residual organic species blocking the Ti species within the channels (Fig. 1B).

The microstructure of the Ti species was monitored with UV–visible spectroscopy during the reaction–regeneration process (Fig. 2). Because the surface was contaminated with the organic species, the used catalyst was pale yellow in color when only washed with acetone, and thus its spectrum showed a broad peak in the region of 300–400 nm (Fig. 2b). Nevertheless, the acetone-washed sample still showed a strong band at 220 nm, assigned to the tetrahedral framework Ti species (11). A weak shoulder around 260 nm was also observed for the acetone-washed sample (Fig. 2b). This band is generally attributed to the octahedral Ti species developed by the coordination of water molecules to the tetrahedral Ti species (17). When the used

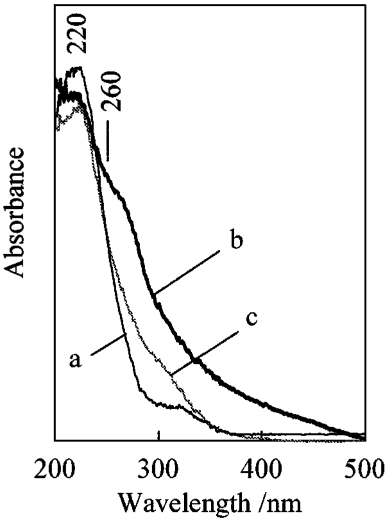

FIG. 2 UV–visible spectra of the fresh Ti–MWW (a), the used catalyst washed with acetone only (b) and the calcined one (c) after 4 reaction–regeneration cycles. The fresh Ti–MWW is No. 3 in Table 1.

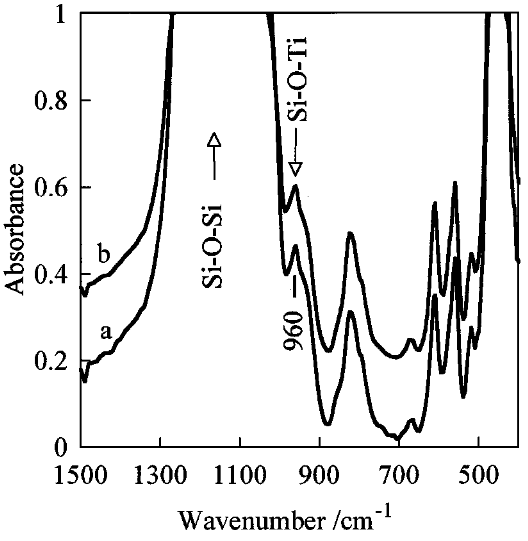

FIG. 3 IR spectra of the fresh Ti–MWW (a) and the used catalysts after calcination in air (b) after 4 reaction–regeneration cycles. The fresh Ti–MWW is No. 17 in Table 1 and the spectra were recorded at room temperature after evacuation at 773 K for 1 h.

catalysts were calcined to remove both the organic species and the adsorbed water, a spectrum nearly the same as that of the fresh catalyst was obtained, even after four cycles of reaction–regeneration (Fig. 2c). The high stability of the Ti species in Ti–MWW was also confirmed by IR spectroscopy. The nearly B-free Ti–MWW sample, No. 17 in Table 1, was used here for the IR measurements to reduce the influence of framework B on observing the stretching band of Si–O–Ti bonds. After calcination, the used catalyst exhibited the characteristic band at 960 cm^{-1} with an intensity comparable to that of the fresh catalysts (Fig. 3). It is reported that a treatment of Ti-Beta with H_2O_2 greatly decreases the intensity of the 960-cm^{-1} IR band and totally converts the 220-nm UV–visible band to a new one at 270 nm, which is further red shift toward the anatase region by subsequent calcination (17). This irreversible behavior indicates less stability of the Ti species in Ti–Beta. Well-crystallized TS-1 generally does not suffer such serious problem. Nevertheless, the byproducts of triols may promote the Ti leaching, especially for TS-1 prepared in a short crystallization period as proposed by Hutchings *et al.* recently (18). Therefore, by combining the literature with the present study, we can conclude that Ti–MWW is at least as stable as TS-1 both in the nature of Ti species and toward the leaching by H_2O_2 and that Ti–MWW shows higher potential in the reutilization than Ti–Beta.

Influence of Framework B on the Catalytic Performance of Ti–MWW

The Al species, required to obtain well-crystallized Ti–Beta, although not so large in the amount, has been shown to greatly retard the intrinsic activity of the framework Ti (3, 4). We have reported that the residual Al in Ti–MOR which is prepared by the $TiCl_4$ treatment on dealuminated mordenite also has a negative influence on the catalytic behavior of the Ti species both in the hydroxylation of toluene and in the ammoximation of cyclohexanone (6b). Since the precursors for preparing Ti–MWW were synthesized by adding a large amount of structure-supporting element of B in the gel, the influence of B on the catalytic properties of the Ti species should be clarified to utilize more effectively the Ti–MWW catalysts.

As shown previously, the B content in the MWW structure can be lowered easily to a nearly B-free level by repeating the acid treatment (11). This allows us to carry out the study on the influence of B. Table 3 compares the catalytic activity of the Ti–MWW catalysts with different B contents. The catalysts used here were prepared from the same sample, i.e., the precursor of Ti–MWW–PI(50), to avoid the

TABLE 3

Comparision of the Catalytic Activity in the Oxidation of Cyclohexene with TBHP for Ti–MWW Catalysts with Different B Content

			Cyclohexene oxidation[b]						
	Composition				Product sel. (mol%)			TBHP (mol%)	
Catalysts[a]	Si/B	Si/Ti	Conv. (mol%)	TON[c]	Oxide	Glycols	Others[d]	Conv.	Sel.
No. 9	39	72	4.2	38	80	9	11	9.3	95
No. 13	543	107	4.0	51	83	3	14	8.8	96
No. 10	89	131	4.5	71	84	6	10	9.5	100
No. 14	553	136	4.4	74	87	2	11	9.6	98

[a] The numbers correspond to those in Table 1. The catalysts were calcined.

[b] Conditions: same as in Table 2.

[c] In mol (mol of Ti)$^{-1}$.

[d] 2-Cyclohexene-1-ol and 2-cyclohexene-1-one.

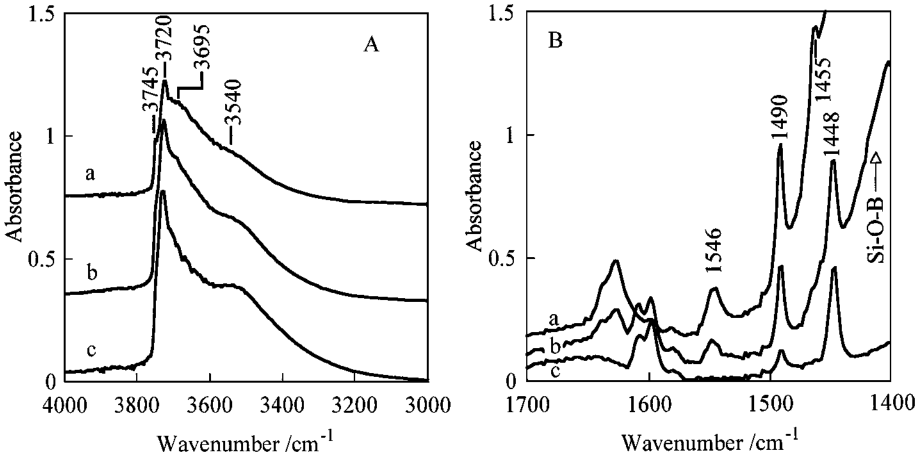

FIG. 4 IR spectra before the pyridine adsorption (A) and after desorption of the adsorbed pyridine at 423 K for 1 h (B) of the directly calcined Ti–MWW–PI(50) (a), No. 9 (b), and No. 13 (c). The numbers correspond to those in Table 1.

possible difference in the nature of Ti species. Table 3 indicates that a decrease in the B content causes an increase in the intrinsic activity of the Ti sites. Nevertheless, taking account of the fact that Al has a detrimental effect on the activity of Ti–Beta in the Si/Al region over 300 (3, 4), and also the fact that Ti–MOR with Si/Al $<$ 100 is essentially inactive (6), with only a slight increase in the TON with decreasing B content, it is hard to draw the conclusion that the B species in Ti–MWW have a significant negative influence on the catalytic activity of the Ti species. Furthermore, as we will show later in this study, the TON of Ti–MMW for bulky reactions falls sharply with the Ti content, which suggests that to obtain accurate information on the influence of the B species, the comparison is required to be carried out at the same Ti level. On this point, the samples of No. 10 and No. 14 with nearly the same Si/Ti ratio showed comparable TON (Table 3). This supports the above hypothesis that the B in Ti–MWW, not like the Al in Ti–Beta and Ti–MOR, does not significantly affect the catalytic activity of the Ti species. The hindrance of Al on the activity of Ti has been attributed to the change in the electronegativity of the zeolite framework in the case of Ti–Beta and Ti–MOR (3, 6). The too small cation radii of B may make the B species loosely incorporated within the SiO_2 framework matrix of the MWW structure and exist probably as the B–OH…HO–Si defect in the hydrated form. The framework B species thus shows less electronegativity and then hardly affects the Ti species than the framework Al. This consideration is supported by the fact that the framework B is easy leached by the acid treatment or even in the aqueous solution (Fig. 1A) while the framework Al in MCM-22 is hardly extracted by the acid treatment as we reported previously (19).

Nevertheless, the framework B atoms may exhibit Brønsted acidity which do not contribute to the oxidation but catalyze the hydrolysis of the oxide product. As shown in Table 3, although the selectivity for the glycols, produced through the ring opening reaction of the oxide product, was generally very low, it decreased with decreasing B content. To further make this issue clear, the IR spectra of adsorbed pyridine were measured to characterize the acidity of Ti–MWW. Figure 4 shows the IR spectra of the Ti–MWW samples containing different B contents before and after the pyridine adsorption. The directly calcined sample of Ti–MWW–PI(50) showed the bands at 3745, 3720, 3695, and 3540 cm^{-1} in the region of a hydroxyl stretching vibration (Fig. 4a). The 3745-cm^{-1} band is ascribed to the terminal silanol groups, while the 3540-cm^{-1} band, showing a broad feature, is due to hydrogen-bonded silanol groups probably on defect sites such as hydroxyl nests (6).

The bands at 3720 and 3695 cm^{-1} may be related to either the silanol groups or the framework B cations. In the case of MFI-type borosilicate, the researchers from different groups assign the band at 3725 cm^{-1} (20) or the band at 3700 cm^{-1} (21) to the structural Si(OH)B groups. The 3720-cm^{-1} band observed for the present Ti–MWW increased in the intensity gradually with the removal of the B (Fig. 4a–c), which favors the assignment of this band to the silanols at defect sites as in the case of highly dealuminated mordenites (6). Therefore, the weak band at 3695 cm^{-1}, showing only a shoulder because of the overlap with the higher frequency band, is probably due to the framework B cations. The removal of B together with Ti left the vacancy in the framework and then increased the intensity of the 3540-cm^{-1} band.

After the adsorption and desorption of pyridine at 423 K, the bands due to the vibration of pyridine ring were observed (Fig. 4B). The band at 1546 cm^{-1} due to pyridium ion and the band around 1450 cm^{-1} due to coordinated pyridine can be taken as evidence of Brønsted and Lewis acid sites, respectively. The 1546-cm^{-1} band decreased in intensity with a decreasing amount of B and totally disappeared for

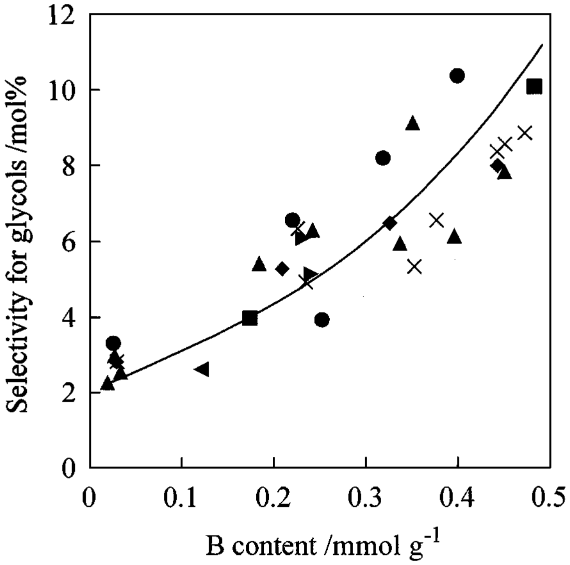

FIG. 5 Dependence of the selectivity for glycols on the B content in the oxidation of cyclohexene with TBHP. Ti–MWW–PI catalysts used were prepared from the lamellar precursors with a Si/Ti ratio of 100 (■), 70 (●), 50 (▲), 30 (◆), 20 (◀), and 10 (▶). Ti–MWW–HM catalysts (×) were prepared from the precursors with a Si/Ti ratio of 100, 70, 50, and 30. For the reaction conditions see Table 2.

the nearly B-free sample, indicating the Brønsted acid sites in Ti–MWW are generated from the framework B cations and can be removed readily by acid treatment. The band around 1450 cm^{-1}, on the other hand, showed no obvious change with the removal of B. The same band with similar intensity was also observed for both the Ti-free samples of Si/B = 11.8 and 694 (not shown). The 1450-cm^{-1} band is thus hardly attributed to the Lewis acid sites generated by the Ti species but probably due to a partial dehydroxylation of the framework species (20b). After evacuation at 523 K for 1 h, all the bands due to pyridine molecules nearly disappeared (not shown), which is consistent with the results of MFI-type borosilicate, indicating that the acid strength of the framework B in Ti–MWW is very weak.

To further investigate the contribution of the acidity to the product distribution, the oxidation of cyclohexene with TBHP was carried out on a series of Ti–MWW catalysts differing in the B content. Figure 5 shows the dependence of the selectivity for glycols on the amount of B; the activity will be discussed in the next section. Although the points were somewhat scattered, a general tendency that the glycol selectivity decreased with a decreasing amount of B can be deduced. This result indicates that the Brønsted acid sites due to the framework B cations catalyze the hydrolysis reaction of cyclohexene oxide to produce glycols. The selectivity for glycols did not fall into zero but remained at the level of 2–3% when the B content decreased to nearly zero. This can be explained by the participation of the acidity related to the silanol groups. As shown in the IR spectra, a high concentration of silanol groups probably at defect sites were developed in the nearly B-free Ti–MWW catalysts (Fig. 4c). These silanol groups, showing weaker acidity than the structural Si(OH)B (19), can also contribute to the ring-opening reaction of the oxide product. This has already been verified for Ti–MCM-41 (9, 10) and Ti–Beta (22) which are abundant in the terminal surface silanol groups.

Clarification of Active Sites in Ti–MWW

Figure 6 shows the dependence of the TON on the amount of Ti in Ti–MWW for the oxidation of cyclohexene with TBHP at 333 K for 2 h. The TON decreased sharply with an increasing amount of Ti for both series of Ti–MWW catalysts. The Ti–MWW–HM catalysts showed slightly lower activity than the Ti–MWW–PI catalysts, which can be attributed to the difference in the crystal size between these two kinds of catalysts as shown in Table 1. The former with a larger crystal size may suffer from a more serious diffusion problem for the bulky reaction than the latter, reasonably showing the smaller TON.

Since the TON was calculated by dividing the amount of cyclohexene converted at a fixed reaction time of 2 h by the Ti amount, the reaction equilibrium if really existing and also the deactivation may account for the behavior observed in Fig. 6. To make this issue clear, we have carried out the kinetic experiments in the oxidation of cyclohexene with H_2O_2, which is also a sterically demanding reaction like the oxidation of cyclohexene with TBHP. Figure 7A shows the conversion for cyclohexene as a function of the reaction time for several representative catalysts. It can be seen that

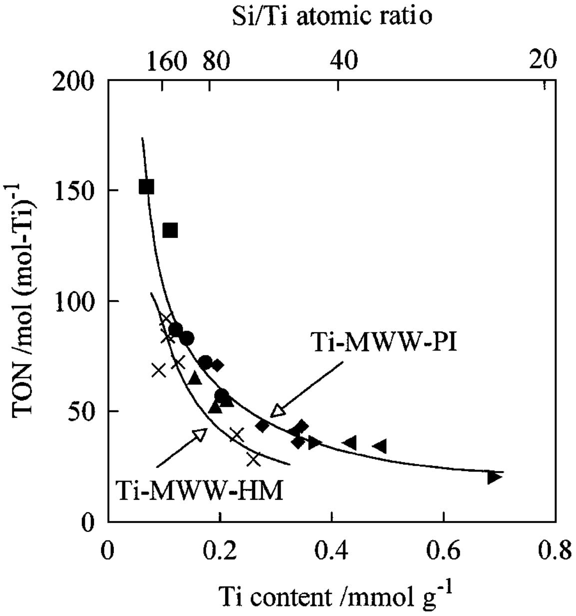

FIG. 6 Dependence of the TON on the Ti content for the oxidation of cyclohexene with TBHP. For symbols and reaction conditions see Fig. 5.

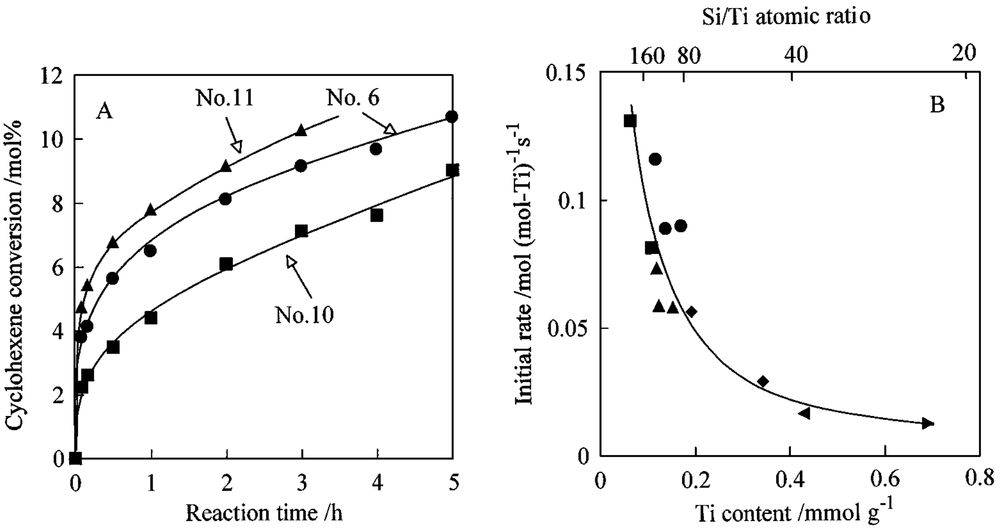

FIG. 7 Change of the cyclohexene conversion with the reaction time (A) and dependence of the initial rate on the Ti content for the oxidation of cyclohexene with H_2O_2. For symbols and the reaction conditions see Fig. 5. The numbers correspond to those in Table 1.

the cyclohexene conversion increased very rapidly at the initial stage and then increased further gradually with the reaction time. The efficiency of H_2O_2 varied between 80 and 100% depending on the catalysts. The initial rate per Ti site was thus obtained and was also plotted against the amount of Ti in Fig. 7B which exhibits a very similar behavior to that observed in the above oxidation with TBHP. Therefore, the reaction equilibrium and the deactivation cannot account for the results observed so far. The presence of nonactive Ti species, e.g., those extraframework Ti species, may be an alternative explanation, but our previous UV–visible and IR data confirmed that nearly all the Ti species are incorporated in the tetrahedral framework sites in the region of Si/Ti over 40 (11). The unusual pore system of the MWW structure may give rise to different Ti species varying in the activity of the size-demanding reactions.

The oxidation of 1-hexene with H_2O_2 thus was conducted to clarify this issue. This reaction is considered to be able to take place on all the Ti species in Ti–MWW because of the relatively small molecular sizes of both the substrate and the oxidant. Table 4 shows the results obtained with Ti–MWW and TS-1. TS-1 showed a TON of 73 for the oxidation of 1-hexene, which was much higher than that for the cyclohexene conversion observed, indicating the Ti species within the 10-ring channels are able to catalyze the present reaction. Ti–Beta, on the other hand, showed little lower activity for the present reaction than that of the oxidation of cyclohexene with H_2O_2. This is accounted for by the low electric density of the terminal C=C bond compared to that of the internal C=C band and consistent with the findings that Ti–Beta is less active than TS-1 for the substrate with no significant diffusion problems within either

TABLE 4

Oxidation of 1-Hexene with H_2O_2 over TS-1 and Ti–MWW

			1-Hexane oxidation[b]					
	Composition				Product sel. (mol%)		H_2O_2 (mol%)	
Catalysts[a]	Si/B	Si/Ti	Conv. (mol%)	TON[c]	Oxide	Diol	Conv.	Sel.
TS-1	∞	104	5.8	73	95	5	6.3	93
Ti–Beta	71[d]	40	8.6	40	97	3	9.8	88
No. 3	34	146	11.3	203	95	5	12.0	94
No. 9	39	72	23.5	222	98	2	25.5	92
No. 18	54	38	44.8	214	99	1	48.2	93

[a] The numbers correspond to those in Table 1. The catalysts were calcined.
[b] Conditions: same as in Table 2 except for H_2O_2, 10 mmol.
[c] In mol (mol of Ti)$^{-1}$.
[d] Si/Al molar ratio.

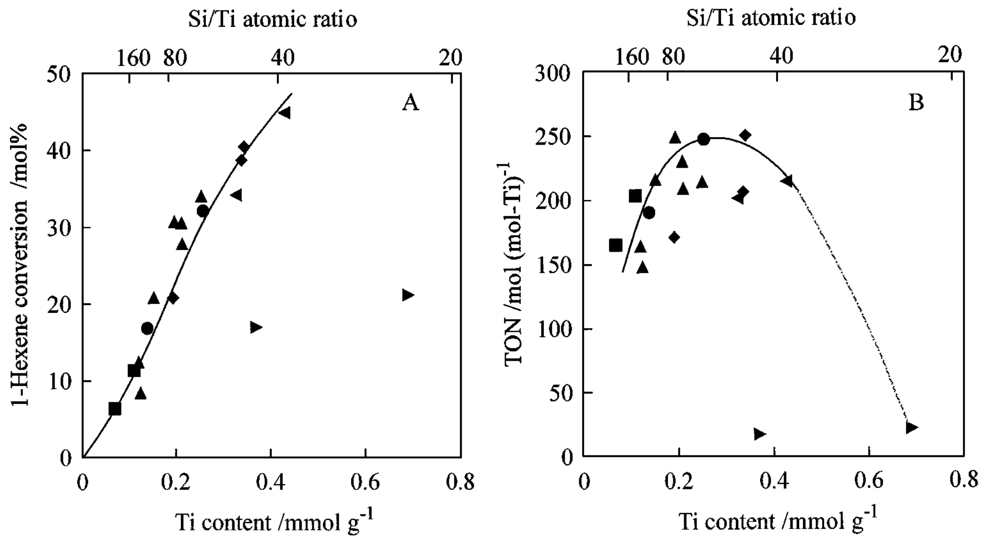

FIG. 8 Dependence of the conversion (A) and the TON (B) on the Ti content for the oxidation of 1-hexene with H_2O_2. For symbols and the reaction conditions see Fig. 5.

MFI or Beta structures (3). It is noteworthy that Ti–MWW catalysts showed much higher activity than either TS-1 or Ti–Beta, indicating that Ti–MWW is an effective catalyst showing high intrinsic activity for small substrates. The selectivity for the oxide product and the efficiency of H_2O_2 for Ti–MWW were generally comparable to that for TS-1. If the conversion for 1-hexene was plotted against the amount of Ti, a good correlation was observed for the Ti–MWW catalysts in the region of Si/Ti $>$ 40 (Fig. 8A). The exception was also observed for several catalysts, especially prepared from the precursors with a Si/Ti ratio of 10, which is ascribed to the presence of a large amount of anatase phase (Table 1). Totally different from that observed for the above bulky reactions, the TON for the 1-hexene conversion showed volcanic behavior (Fig. 8B).

By combining all the above results, we can summarize graphically here the Ti active sites corresponding to the different types of oxidation reactions over Ti–MWW (Scheme 2). Bulky reactions such as the oxidation of cyclohexene with TBHP or H_2O_2 should be catalyzed mainly by the Ti species within the pockets on the crystal surface (Ti site 1) and those within the supercages (Ti site 2). This is because the Ti species of both site 1 and site 2 are more accessible to large substrates. However, besides the Ti site 1 and 2, those within the 10-ring channels (Ti site 3) also show the contribution to the less sterically demanding reaction, e.g., the oxidation of 1-hexene with H_2O_2. If the Ti sites located in different positions are assumed to have the same catalytic ability for the reaction without any diffusion problem, the same TON would be expected for the Ti–MWW catalysts, even with different Ti contents provided that all the Ti species are tetrahedrally incorporated in the framework. In contrast, the Ti–MWW catalysts showed a gradual increase in the TON in the region of low Ti content, even for the reaction of nonbulky 1-hexene (Fig. 8B). The 10-membered channels are not only narrower in size but also longer because they are running along the *ab* planes. Thus, they are reasonably suggested to suffer from serious steric hindrance for the intermediate of Ti peroxo than the surface pockets and the supercages. Therefore, it follows that the distribution of the Ti sites within the crystals can also affect the activity of Ti–MWW. We have shown with UV–visible spectra that during hydrothermal synthesis the Ti

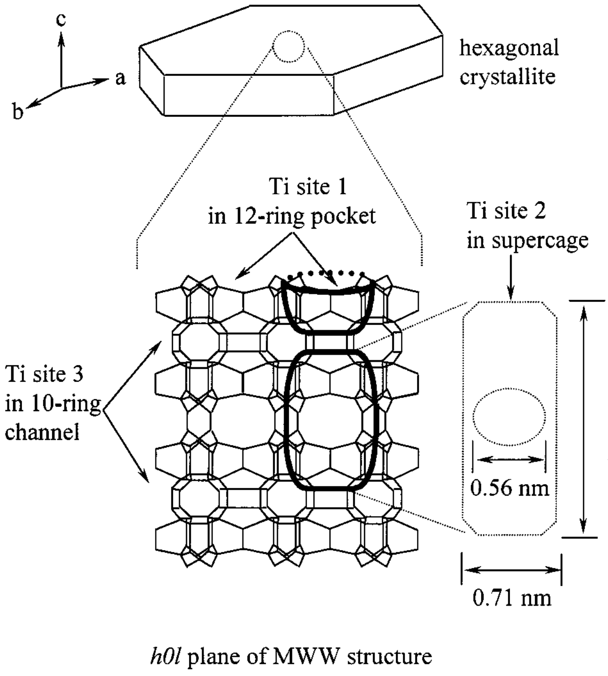

SCHEME 2

species take the advantage of occupying first the tetrahedral sites in the framework and then the octahedral sites on the exterior of the sheets when increasing the Ti content in the gel (11). This suggests a possible gradient of the Ti concentration from the inner crystal to the surface, that is, Ti richness within the inner crystals, and then the possibility of Ti richness in the 10-membered ring channels at low Ti content level. This can explain the increasing behavior of the TON for 1-hexene in the region of relatively low Ti content. The sharp decrease in the TON below Si/Ti = 40 is simply due to the increase in nonactive anatase species on the catalysts.

CONCLUSION

Ti–MWW, prepared from a Ti-containing lamellar precursor after removal of the extraframework Ti species by acid treatment, is a catalyst superior to TS-1, Ti–MOR, and Ti–MCM-41 for the oxidation of alkenes with either H_2O_2 or TBHP at the same experimental conditions and exhibits comparable activity to Ti–Beta for a bulky reaction such as the oxidation of cyclohexene with TBHP. Such unusual activity of Ti–MWW is due to its high stability in both the structure and the nature of the framework Ti species, little negative influence of the residual B species on the catalytic performance of the Ti species, and more importantly the unique structure of the MWW topology. The supercages within the crystals and the exterior pockets directly related to the crystal form of the thin platelets make the Ti species in Ti–MWW highly accessible to both the bulky substrate and the bulky oxidant. Although the 10-membered ring channels within the thin sheets are not accessible to the bulky substrates, they can allow sterically less demanding small reactions such as the oxidation of 1-hexene with H_2O_2 to occur, resulting in high activity of Ti–MWW.

REFERENCES

1. Bellussi, G., and Rigguto, M. S., *Stud. Surf. Sci. Catal.* **85**, 177 (1194).
2. Notari, B., *Adv. Catal.* **41**, 253 (1996).
3. (a) Camblor, M. A., Corma, A., Martínez, A., and Pérez-Pariente, J., *J. Chem. Soc. Chem. Commun.* 589 (1992). (b) Corma, A., Camblor, M. A., Esteve, P., Martínez, A., and Pérez-Pariente, J., *J. Catal.* **145**, 151 (1994). (c) Corma, A., Esteve, P., Martínez, A., and Valencia, S., *J. Catal.* **152**, 18 (1995).
4. (a) Tatsumi, T., Xia, Q. H., and Jappar, N., *Chem. Lett.* 677 (1997). (b) Jappar, N., Xia, Q. H., and Tatsumi, T., *J. Catal.* **180**, 132 (1998). Tatsumi, T., and Jappar, N., *J. Phys. Chem.* **102**, 7126 (1998).
5. Tule, A., *Zeolites* **15**, 236 (1995).
6. (a) Wu, P., Komatsu, T., and Yashima, T., *J. Phys. Chem.* **100**, 10316 (1996). (b) Wu, P., Komatsu, T., and Yashima, T., *J. Catal.* **168**, 400 (1997). (c) Wu, P., Komatsu, T., and Yashima, T., *Stud. Surf. Sci. Catal.* **105**, 663 (1997). (d) Wu, P., Komatsu, T., and Yashima, T., *J. Phys. Chem. B* **102**, 9297 (1998).
7. Diaz-Cabanas, M., Villaescusa, L. A., and Camblor, M. A., *Chem. Commun.* 761, 2000.
8. Corma, A., *Chem. Rev.* **97**, 2373 (1997).
9. (a) Tatsumi, T., Koyano, K. A., Tanaka, Y., and Nakata, S., *Stud. Surf. Sci. Catal.* **117**, 143 (1998). (b) Tatsumi, T., Koyano, K. A., and Igarashi, N., *Chem. Commun.* 325 (1998).
10. Corma, A., Domina, M., Gaona, J. A., Jordá, J. L., Navarro, M. T., Rey, F., and Pérez-Pariente, J., *Chem. Commun.* 2211 (1998).
11. (a) Wu, P., Tatsumi, T., Komatsu, T., and Yashima, T., *Chem. Lett.* 774 (2000). (b) Wu, P., Tatsumi, T., Komatsu, T., and Yashima, T., *J. Phys. Chem. B* **105**, 2897 (2001).
12. (a) Leonowicz, M. E., Lawton, J. A., Lawton, S. L., and Rubin, M. K., *Science* **264**, 1910 (1994). (b) Lawton, S. L., Leonowicz, M. E., Partridge, P. D., Chu, P., and Rubin, M. K., *Microporous Mesoporous Mater.* **23**, 109 (1998).
13. Roth, W. J., Kresge, C., Vartuli, J. C., Leonowicz, M. E., Fung, A. S., and McCullen, S. B., *Stud. Surf. Sci. Catal.* **94**, 301 (1995).
14. Corma, A., Fornés, V., Pergher, S. B., Maesen, Th. L. M., and Buglass, J. G., *Nature* **396**, 353 (1998).
15. Blasco, T., Corma, A., Navarro, M. T., and Pérez-Pariente, J., *J. Catal.* **156**, 65 (1995).
16. (a) Bellussi, G., Carati, A., Clerici, M. G., Maddinelli, G., and Millini, R., *J. Catal.* **133**, 220 (1992). (b) Clerici, M. G., Ingallina, P., *J. Catal.* **140**, 71 (1993). (c) Clerici, M. G., Ingallina, P., and Millini, R., *in* "Proceedings of the 9th International Zeolite Conference" (R. von Ballmoos, *et al.*, Eds.), p. 445. Butterworth-Heinemann: Woburn, MA, 1993.
17. Carati, A., Flego, C., Previde Massara, E., Millini, R., Carluccio, L., and Bellussi, G., *Microporous Mesoporous Mater.* **30**, 137 (1999).
18. (a) Davies, L., McMorn, P., Bethell, D., Page, P. C. B., King, F., Hancock, F. E., and Hutchings, G. J., *Chem. Commun.* 1807 (2000). (b) Davies, L., McMorn, P., Bethell, D., Page, P. C. B., King, F., Hancock, F. E., and Hutchings, G. J., *Phys. Chem. Chem. Phys.* **3**, 632 (2001).
19. Wu, P., Komatsu, T., and Yashima, T., *Microporous Mesoporous Mater.* **22**, 343 (1998).
20. Chu, C. T.-W., and Chang, C. D., *J. Phys. Chem.* **89**, 1569 (1985).
21. (a) Sayed, M. B., and Védrine, J. C., *J. Catal.* **101**, 43 (1986). (b) Coudurier, G., Auroux, A., Védrine, J. C., Farlee, R. D., Abrams, L., and Shannon, R. D., *J. Catal.* **108**, 1 (1987).
22. Camblor, M. A., Costantini, M., Corma, A., Gilbert L., Esteve, P., Martínez, A., and Valencia, S., *Chem. Commun.* 1339 (1996).